Quantifying the effect of electronic conductivity on the rate-performance of nanocomposite battery electrodes

Journal:	*ACS Applied Energy Materials*
Manuscript ID	ae-2020-00034s.R2
Manuscript Type:	Article
Date Submitted by the Author:	30-Jan-2020
Complete List of Authors:	Tian, Ruiyuan; Trinity College Dublin, School of Physics and CRANN Alcala, Nolito; Dublin Institute of Technology O'Neill, Steven; University of Dublin Trinity College, Physics Horvath, Dominik; University of Dublin Trinity College, Physics Coelho, João; Trinity College Dublin, Griffin, Aideen; University of Dublin Trinity College, Physics Zhang, Yan; University College Cork Nicolosi, Valeria; University of Dublin Trinity College, School of Chemistry, School of Physics & CRANN O'Dwyer, Colm; University College Cork National University of Ireland, School of Chemistry Coleman, Jonathan; University of Dublin Trinity College, Physics

Quantifying the effect of electronic conductivity on the rate-performance of nanocomposite battery electrodes

Ruiyuan Tian,[1,2*] Nolito Alcala,[3] Stephen JK O'Neill,[1,2] Dominik Horvath,[1,2] João Coelho,[2,4] Aideen Griffin,[1,2] Yan Zhang,[5] Valeria Nicolosi,[2,4] Colm O'Dwyer,[2,5] Jonathan N Coleman[1,2]*

[1]*School of Physics, Trinity College Dublin, Dublin 2, Ireland*

[2]*AMBER Research Center, Trinity College Dublin, Dublin 2, Ireland*

[3]*School of Physics, Technological University Dublin, City Campus, Kevin Street, D08 NF82, Ireland*

[4]*School of Chemistry, Trinity College Dublin, Dublin 2, Ireland*

[5]*School of Chemistry, University College Cork, Tyndall National Institute, and Environmental Research Institute, Cork T12 YN60, Ireland*

*rtian@tcd.ie (Ruiyuan Tian); colemaj@tcd.ie (Jonathan N. Coleman); Tel: +353 (0) 1 8963859.

ABSTRACT: While it is well-known that electronic conductivity of electrodes has a critical impact on rate-performance in batteries, this relationship has been quantified only by computer simulations. Here we investigate the relationship between electrode electronic conductivity and rate-performance in a model system of Lithium-Nickel-Manganese-Cobalt-Oxide (NMC) cathodes filled with various quantities of carbon black, single-walled carbon nanotubes and graphene. We find extreme conductivity anisotropy and significant differences in the dependence of conductivity on mass fraction among the different fillers. Fitting capacity versus rate curves yielded the characteristic time associated with charge/discharge. This parameter increased linearly with the inverse of the out-of-plane electronic conductivity, with all data points falling on the same master curve. Using a simple mechanistic model for the characteristic time, we develop an equation which matches the experimental data almost perfectly with no adjustable parameters. This implies that increasing the electrode conductivity improves the rate-performance by decreasing the RC charging time of the electrode and shows rate performance to be optimised for any electrode once σ_{OOP}>1 S/m, a condition achieved by including <1wt% single-walled carbon nanotubes in the electrode.

Keywords: anode; cathode; rate-limitations; analytic model; electrical limitations

1. INTRODUCTION

Rechargeable batteries based on the storage of Lithium ions are becoming more and more important for many applications including electric vehicles, mobile electronics and even large-scale energy storage.[1-2] While much of the focus within the research community has been on maximising capacity and energy density, often through the use of novel materials,[3-5] somewhat less attention has been given to optimising rate-performance.[6] Nevertheless, achieving high rate-performance is critical to achieving rapid charging or high power delivery in a range of applications.[7]

It is well known that many factors affect the rate-performance of an electrode/electrolyte system, including the solid-state diffusion time, the time taken for ions to diffuse within the electrolyte and the ability of the electrode material to rapidly distribute charge.[8-12] This latter factor generally requires intervention as many battery materials have relatively low electronic conductivity. To address this, conductive additives are almost always incorporated into the electrode to reduce electrode resistance.[13] In most cases, tried and tested formulations are used, with the addition of ~10wt% carbon black being particularly common.

However, there does not seem to be a clear rule defining the aims associated with incorporating the conductive additives. For instance, it would be useful to know exactly what minimum electronic conductivity is being targeted. This would allow one to minimise the conductive additive content, thus maximising the active material content, while still reaching the target conductivity for optimizing rate performance. In addition, the literature does not generally contain much discussion as to what aspect of electronic conductivity is important. For example, films containing networks of conducting nano-carbons, especially those cast from liquids, can be very anisotropic, leading to significant differences between in-plane and out-of-plane electronic conductivity.[14-15] Although the in-plane conductivity is easy to measure and is often reported,[16-17] the out-of-plane conductivity is probably more relevant in battery electrodes as it governs transport of charge from current collector to active sites.[12] Indeed, it has been shown that the out-of-plane conductivity corresponds very well to the electrode resistance measured by impedance spectroscopy.[18] However, we are aware of no quantitative examination of the relationship between either in-plane or out-of-plane electronic conductivity and rate-performance. Such a relationship would be extremely useful as it would allow the identification of the minimum electronic conductivity required to optimise rate-performance.

In this work we study both the in-plane and out-of-plane conductivities of battery electrodes based on NMC filled with three different nano-fillers, carbon black (CB), single-walled carbon nanotubes (CNT) and graphene (Gra), at various loadings. While we find both in-plane and out-of-plane electronic conductivities to scale with filler volume fraction as per percolation theory, the out-of-plane conductivity was roughly three orders of magnitude lower that that measured in-plane. Rate measurements showed the characteristic time associated with charge/discharge to scale inversely with out of plane conductivity. Using a simple mechanistic model, we can match the data almost perfectly with no adjustable constants. Then, using the model, we show rate-performance optimisation to occur in almost all circumstances once the out-of-plane electronic conductivity exceeds 1 S/m.

2. RESULTS AND DISCUSSION

Electronic conductivity of electrodes

We produced a range of electrodes of NMC, loaded with varying mass fractions (M_f) of CNTs ($0.01\%<M_f<4\%$), graphene ($0.1\%<M_f<30\%$) and carbon black ($0.1\%<M_f<20\%$). In each case, we were careful to measure areal mass (M/A) and thickness (L_E) of the electrodes, allowing us to calculate their density (ρ_E) and porosity (P_E) as well as filler volume fraction (ϕ). In general, the electrodes were ~100 μm thick with mass loadings of ~15 mg/cm^2. The electrode density tended to vary from 2.2-1.5 g/cm^3, depending on the filler and loading (see SI). SEM images (figure 1) show the electrodes to consist of loosely packed disordered arrays of NMC particles (diameter ~5-15 μm) surrounded by a lose network of filler particles. Such a system where the matrix (i.e. active) particles are larger than the filler (i.e. CB, CNT or graphene) particles is called a segregated network and has been shown to result in high conductivities at relative low filler mass fractions.[18-19]

For each electrode, we measured both the in-plane (IP) and out-of-plane (OOP) apparent electronic conductivity using the two-probe technique as described in methods. We use the term apparent conductivity as two probe techniques include the effects of contact resistance which can have a significant impact when the material resistance is small. While contact resistance effects can be removed by using 4-probe measurements, this is not straightforward for OOP measurements. In composites, conductivities are usually analysed in terms of filler volume fraction, ϕ, rather than M_f. The volume fraction can be calculated from $\phi = M_f \rho_E / \rho_{filler}$, which is found by defining $\phi = V_{filler} / V_{electrode}$.[15]

Shown in figure 2A-C are both in-plane (σ_{IP}) and out-of-plane (σ_{OOP}) electronic conductivities for composites with CB (A), graphene (B) and CNT fillers (C), all as a function of ϕ. In each case, the conductivity increases rapidly with ϕ, once a minimum filler volume fraction had been surpassed. For all materials, the maximum IP conductivity was ~1000 S/m while the highest OOP conductivity observed was ~0.1 S/m. Over all filler loadings, the in-plane conductivity was between ×4 and ×3000 larger than σ_{OOP}. Such large conductivity anisotropies have been observed before for nanostructured networks[14-15, 20-21] and occur when the networks are partially aligned in the plane of the film, and also common for predominantly layered or vdW materials in composite and non-composite, thin film formats. Such electronic conductivity anisotropy will have significant implications for performance in battery electrodes because measurement of in-plane conductivity will significantly over-estimate the effect of the conductivity on rate-performance. Unusually for such composites, both in-plane and out-of-plane conductivities saturated for the nanotube filled composites as the volume fraction surpassed ~0.2%.

For composites filled with conductive additives, the electronic conductivity is described by percolation theory. Within this model, the conductivity increases only above a critical volume fraction where the first complete conductive path is formed, a value known as the percolation threshold, ϕ_c. Above this threshold, the composite conductivity, σ, scales as:

$$\sigma = \sigma_0(\phi - \phi_c)^t \quad (1)$$

where σ_0 is a constant related to the conductivity of the filler network and t is the percolation exponent.[15, 22]

With this in mind, it is clear that the percolation threshold for CB and graphene composites is ~1-2vol% but much lower for the nanotube-filled composites. Equation (1) fits the data extremely well for the CB and graphene composites in both IP and OOP directions with all fit parameters given in table 1. The percolation thresholds are very similar between IP and OOP directions indicating that network connectivity is similar in the in-plane and out-of-plane directions. The in-plane percolation exponents were close to the universal, 3-dimensional value of 2.0 which indicates that the distribution of inter-particle junction resistances is fairly narrow.[15] However, OOP exponents were slightly lower, perhaps due to network alignment effects.[23] However, the major difference between IP and OOP parameters for the CB and graphene samples were the σ_0 values which were approximately ×1000 higher in the IP

direction. Such a large anisotropy confirms that the conducting networks are significantly aligned in the plane of the electrode.

However, the σ-ϕ curves for the nanotube-filled samples behaved differently, saturating at higher loadings. We can explain this by noting that, for two-probe measurements, the measured resistance is the sum of composite and contact resistance (R_C). Converting these resistances to conductivity via the electrode area, A, and separation, L, yields the effective (ie measured) conductivity

$$\sigma_E = \frac{1}{(R_C A / L) + 1/\sigma} \quad (2a)$$

where σ is the intrinsic composite conductivity. We can use equation (1) to replace σ, yielding:

$$\sigma_E = \frac{1}{(R_C A / L) + \left[\sigma_0 (\phi - \phi_c)^t\right]^{-1}} \quad (2b)$$

We note that when the contact resistance is very small, equation (2b) reverts to equation (1). We find equation (2b) fits the data extremely well. As shown in table 1, the exponents are very similar to the other materials. However, the percolation thresholds are considerably lower while the σ_0 values are much higher than the CB and graphene-based composites. Taken together, this means carbon nanotubes yield much higher conductivities at lower loading levels compared to other fillers.

The superiority of nanotubes, both in terms of percolation threshold and σ_0 is striking and probably due to their high aspect ratio. Although individual single walled nanotubes of the type used here are similar in length (~5 μm) to the upper end of the graphene nanosheet length distribution (1-5 μm), they have a significant advantage in that they tend to self-assemble into extremely long (up to ~100 μm) bundles.[15] Such bundles are very conductive and, when used in nano-nano composites such as these, yield high conductivities at low loading.[18] Perhaps the biggest surprise here is that the graphene-filled composites are so much closer to those filled with CB than CNT. However, this may simply be a geometric issue and a signal that nanosheets are not as well suited to segregated network formation as CNT, perhaps due to aggregation effects.[24] Indeed previous work on MXene nanosheet/silicon nanoparticle composites have shown relatively high loadings of ~30wt% MXenes are required to achieve in-plane conductivities >1000 S/m.[19]

In addition, we use the fits to estimate the contact resistances, R_CA, for the CNT-filled composites. These work out to be 9×10^{-6} Ωm^2 and 3.3×10^{-4} Ωm^2 for the IP and OOP directions. This difference is to be expected based on the nature of the contacts (see methods), with the top contact in the OOP measurement being relatively poorly connected to the electrode.

Once we know σ_0, ϕ_c and n for the CNT-filled electrodes, it is possible to estimate the composite conductivity (i.e. neglecting contact effects) as a function of volume fraction, ϕ, using equation (1). We have plotted equation (1) on figure 2C (solid lines) using the fit parameters given in table 1. These curves confirm that the true composite conductivities for nanotube-filled electrodes can be significantly higher than for the other systems.

Measuring rate performance

This work shows clearly that the out-of-plane electronic conductivity of these electrodes is significantly lower than the in-plane electronic conductivity and varies greatly depending on filler. Because it controls transport of charge from current collector to Li storing sites, we would expect the OOP conductivity to directly impact the electrodes rate-performance. As a result, it is worth measuring capacity-rate data for each composite type at a number of filler loadings with the aim of correlating rate-performance with σ_{OOP}. We make the assumption here that each electrode is electrolyte-saturated and there is no preference for Li^+ accessibility to the surface of active materials in all cases, aside from cation diffusion within the electrolyte. We further assume that changing the filler does not significantly affect rate performance via factors such as porosity and charge transfer resistance. This will be discussed in more detail below.

We fabricated electrodes based on NMC with various mass fractions of CB, graphene and CNT in the same way as described above. First, we performed galvanostatic charge discharge (GCD) measurements to check the electrodes were performing correctly. As shown in the SI, in all cases, the GCD curves are consistent with previous reports,[25] with the capacity increasing somewhat with filler loading as expected.[16] Normally, rate-performance measurements are carried out by performing GCD measurements at a range of specific currents. However, such measurements are slow, limiting the ability to rapidly and accurately characterise a large number of electrodes, especially when quantitative analysis requires many rate measurements per sample. To get around this problem, we used a recently reported, relatively rapid method of making rate measurements: chronoamperometry (CA).

Heubner et al.[26] have shown that CA is a very effective technique for performing rate-performance measurements. This method has the advantages that it is quicker than GCD and yields many more data points down to lower rates. In practice, a potential step is applied to the

electrode and the current transient measured. Heubner et al. published equations to transform the I(t) data into capacity as a function of C-rate.

However, we have previously argued that quantitative analysis of rate-performance measurements is better performed on plots of capacity versus charge/discharge rate, R where R is defined as[12]

$$R = \frac{I/M}{(Q/M)_E} \tag{3}$$

Where I/M is the specific current (current per unit mass) and $(Q/M)_E$ is the measured experimental specific capacity, rather than the theoretical value. In this way, R is related to the actual charge/discharge time. We have shown that the CA current transient can be converted to specific capacity, Q/M, and R using:[27]

$$R = \frac{I(t)/M}{\int_0^t (I(t)/M)dt} \tag{4a}$$

and

$$Q/M = \int_0^t (I(t)/M)dt \tag{4b}$$

where we note that, in this paper, all specific capacities are normalised to the active mass. We have shown that these equations give capacity-rate curves which match extremely well to those obtained by GCD.[27] However, they can be measured in approximately one third of the time.

Presented in figure 3 are Q/M vs. R curves for each of the three composite types for three different mass fractions of carbon-base conductive additives. The first thing to note is that the CA-derived curves have the same shape as standard GCD-derived rate curves. The main difference is the much higher data density. Secondly, these curves clearly show both the rate-performance and the low-rate capacity to increase with filler loading as expected.

Fitting rate data

In order to quantitatively analyse the relationship between rate-performance and electrode electronic conductivity, it is necessary to extract a number from each capacity-rate graph which quantifies the rate-performance. Recently,[12] we proposed a semi-empirical equation for fitting capacity-rate data which outputs three fit parameters to assess rate-performance:

$$\frac{Q}{M} = Q_M\left[1-(R\tau)^n\left(1-e^{-(R\tau)^{-n}}\right)\right] \tag{5}$$

Here Q_M is the specific capacity at very low rate, τ is a time constant associated with charge/discharge and is a measure of the rate at which *Q/M* starts to fall off.[12, 28] This parameter is particularly important as low time constants mean fast charge/discharge and indicate good rate-performance. Finally, *n* is an exponent describing how rapidly *Q/M* decays at high rate with diffusion-limited electrodes showing n~0.5 while capacitive-limited (i.e electrically limited) electrodes yield n~1.[12] Knowledge of *n* and especially τ allows a proper, quantitative assessment of the rate-performance of a given electrode.

We have used equation (5) to fit all of our Q/M vs. R curves with examples of fits shown in figure 3. In all cases the fits were very good giving us confidence in the accuracy of the fit values. These fit values are plotted versus filler mass fraction in equation (5) for each composite type. While Q_M is not an indicator of rate-performance, we plot it in figure 4A to confirm the results to be as expected. In line with previous results, we find the low-rate capacity to increase with mass fraction of conductive filler.[16] Interestingly, the capacity increases occur at much lower mass fractions for the nanotube-filled samples compared to the CB- and graphene-filled electrodes, simply due to their lower percolation threshold (figure 2). The exponent, n, is plotted versus M_f in figure 4B. For low mass fractions, n is closer to 1 than 0.5 in all cases, consistent with these electrodes being predominately electrically limited (i.e. limited by the RC charging time of the electrode).[12, 27] However, in each case, n appears to fall slightly with filler loading. This is consistent with increasing conductivity reducing the resistance of the system, thus slightly shifting the rate-limiting effect from electrically- to diffusion-limited.[12] For low mass fractions of conductive additive, high internal resistance limits the rate of electrochemical reduction of the available Li^+. However, as the conductive additive loading is increased, the internal resistance falls and the rate of arrival of Li^+ becomes limiting. We would expect that, for thick electrodes such as these (~100 μm), one the electronic conductivity is high enough, the main ion transport limitation is diffusion within the electrolyte within the porous interior of the electrode.[12]

However, most important for rate-performance is the characteristic time, τ. This parameter is a measure of the rate, above which capacity begins to fall off. As such it can be thought of as approximately the minimum charge/discharge time where the full low-rate capacity can be achieved. As such, this parameter nicely quantifies rate-performance with better performance associated with low τ. As shown in figure 4C, in all cases τ falls with filler M_f, behaviour which has been observed previously.[12] Interestingly, the nanotube-filled composites reach lower

values of τ at much lower loadings compared to the other two materials. This would suggest carbon nanotubes to be the best fillers when rate-performance is concerned, in terms of their ability to minimise τ at low mass fraction.

Mechanistic analysis

We can understand these results by considering a model which we recently reported that describes τ in terms of the various timescales associated with ion motion in the system.[12] There are three main contributions to τ: the RC time constant of the system, the timescale associated with diffusion and the time associated with the electrochemical reaction. Each of these contributions can be broken into one or more terms within the equation. The RC terms include contributions from the electrical resistance of the electrode (term 1) as well as the ionic resistances of the electrolyte within the pores of the electrolyte (term 2) and within the separator (term 4). The diffusive terms include contributions from the times required for ions to diffuse through the electrolyte-filled porous interior of the electrode (term 3), the time required to diffuse through the separator (term 5) and the solid-state diffusion time (term 6). The final term (7) describes the timescale associated with the electrochemical reaction, t_c.

This yields the following equation[12]

$$\tau = L_E^2\left[\frac{C_{V,eff}}{2\sigma_{OOP}} + \frac{C_{V,eff}}{2\sigma_{BL}P_E^{3/2}} + \frac{1}{D_{BL}P_E^{3/2}}\right] + L_E\left[\frac{L_S C_{V,eff}}{\sigma_{BL}P_S^{3/2}}\right] + \left[\frac{L_S^2}{D_{BL}P_S^{3/2}} + \frac{L_{AM}^2}{D_{AM}} + t_c\right] \qquad (6a)$$

Term 1 2 3 4 5 6 7

Here $C_{V,eff}$ is the effective volumetric *capacitance* of the electrode, σ_{OOP} is the out-of-plane electronic conductivity of the electrode material, P_E and P_S are the porosities of the electrode and separator respectively while L_S is the separator thickness. Here σ_{BL} is the overall (anion and cation) ionic conductivity of the bulk electrolyte (S/m) while D_{BL} is the ion diffusion coefficient in the bulk electrolyte. In addition, L_{AM} is the solid-state diffusion length associated with the active particles (related to particle size); D_{AM} is the solid-state Li ion diffusion coefficient within the particle. We note that the volumetric capacitance of a battery electrode may not be known. However, we have shown empirically that $C_{V,eff}$ is directly proportional to the low-rate total (i.e. normalised to total electrode volume) volumetric capacitance of the electrode, Q_V, which applies over a range of electrode materials, such that: $C_{V,eff} / Q_V = 28$ F/mAh is a general relation.[12]

We note that equation 6a differs from most simple capacity-rate models which generally only consider only diffusion limitations, usually in the electrolyte but also in the solid, Li-storing material.[29] To our knowledge, equation 6a is the only quantitative model which incorporates the effects of electrode electronic conductivity on capacity-rate behaviour.

Here, we are interested in the dependence of τ on σ_{OOP}. In figure 5A we plot τ versus σ_{OOP} for all three materials. We note that for the high CNT loading levels, we used figure 1, combined with the percolation fit parameters, to estimate the composite electronic conductivity, removing the contribution of contact resistance. We find τ to fall significantly with increasing σ_{OOP}.

We can understand this behaviour by combining equation (6a) with the empirical relationship between $C_{V,eff}$ and Q_V yielding:

$$\tau = \frac{14 Q_V L_E^2}{\sigma_{OOP}} + \beta \qquad (6b)$$

where β is just shorthand for terms 2-7 and Q_V should be expressed in mAh/m^3. This equation implies that τ should scale linearly with $1/\sigma_{OOP}$. As shown in figure 5A inset, we find this relationship to describe the data reasonably well, albeit with some scatter.

We should not be surprised that the data in figure 5A is slightly scattered because, as shown in figure 4A, Q_M shows a non-trivial variation over the samples. This means Q_V, which appears in equation (6b) will also vary (because $Q_V \propto Q_M$). In addition, there are small unavoidable variations in the electrode thickness, L_E, over the samples (variation from 68-140 μm, mean 97 μm, std dev 18 μm). To combat these problems, we rearrange equation (6b) slightly to read.

$$\frac{\tau}{L_E^2} = 14 \frac{Q_V}{\sigma_{OOP}} + \frac{\beta}{L_E^2} \qquad (7)$$

This implies that a graph of τ / L_E^2 vs. Q_V / σ_{OOP} should be a straight line with a slope which is material independent at 14 F/mAh. To plot this graph, we use our electrode density measurements to calculate Q_V for each electrode using $Q_V = f_{Active} \rho_E Q_M$, where f_{Active} is the mass fraction of active material within the electrode (this factor is required because Q_M is normalised to active mass while Q_V is normalised to total electrode mass). This graph is presented in figure 5B and shows a very well-defined straight line with reduced scatter compared to the data in figure 5A.

To test for quantitative agreement, we do not fit the data using equation (7). Instead, we directly plot equation (7) on figure 5B. The model predicts that the slope of this plot be 14 F/mAh while the intercept, β / L_E^2, can be found by using reasonable values of the electrode parameters in terms 2-7 of equation (6a). The parameters used are given in the caption of figure 5B (and are justified in the SI) and yield a value of the intercept to be $\beta / L_E^2 = 3.5\times10^{10}$ S/m^2. Plotting equation (7) using this slope and intercept gives the solid line in figure 5B.

We find the agreement between the plot of equation (7) and the data in figure 5B remarkable. Such agreement between experiment and theory has a number of implications. First it strongly supports the validity of the model represented by equation (6a). Using the CA method also implies that a suitable voltage range is used such that the correlation in values between the CA approach using the lower voltage limit, and the capacity obtained from GCD, are comparably precise for these electrodes. This is important as it gives us confidence that the model can be used to analyse data or to predict behaviour. Secondly, the slope of equation (7) is determined by the empirical relationship between electrode volumetric capacity and volumetric capacitance reported in ref[12]. The almost perfect match between the slopes of model and data in figure 5B strongly supports this empirical relationship. It furthermore identifies the sensitive dependence on σ_{OOP} even when all primary diffusion limitations for the intercalation reactions (electrode and electrolyte) are considered. This data also confirms that it is the out-of-plane electrode electronic conductivity that determines rate behaviour (rather than σ_{IP}), even for randomly mixed composites.

In addition, it is worth noting that changing the conductive additive could lead to some variations in the morphology and the microstructure of the composite. Such changes might effect rate performance via factors such as charge transfer resistance[30] or the effect of porosity/tortuosity on ionic mobility.[12, 31] Such changes would certainly alter τ, for example via term 7 which would be effected by changes in charge transfer resistance and terms 2 and 3 which depend on ionic mobility. However, any significant changes in these terms would alter τ to the point where the data in figure 5B for the different composite types would no longer sit on the same master curve. That the data does indeed sit on the same curve, consistent with a common intercept, indicates that (here at least) changing the filler doesn't significantly affect rate-limiting factors other than electronic conductivity.

In the literature, trial and error has led to a number of much-used electrode formulations (e.g. using 10wt% CB) which give high electrode OOP conductivities, such that term 1 in equation

6a is probably negligible in most cases. It is worth noting that we can clearly see the effect of term 1 in figure 5B (i.e. the linear increase in τ / L_E^2) because we have effectively reduced the electrode electronic conductivity by using artificially low levels of conductive additive content.

Predicting minimum required electrode conductivities.

The data in figure 5A suggests that, at least for the electrodes under study here, the time constant is minimised once σ_{OOP} exceeds about 1 S/m. This occurs because once σ_{OOP} gets large enough, term 1 in equation (6a) becomes negligible compared to the rest of the terms. We can use this idea to identify the minimum electrode electronic conductivity required to render term 1 negligible for any electrode. We can do this by imposing the (somewhat arbitrary) condition that term 1 becomes unimportant when it falls below 10% of the sum of the other 6 terms. Expressing this condition and then rearranging gives an expression for the minimum out-of-plane electronic conductivity required to optimise rate-performance (with respect to filler content) by eliminating term 1:

$$\sigma_{OOP,Min} = \frac{14Q_V}{0.1\left[\frac{14Q_V}{\sigma_{BL}P_E^{3/2}} + \frac{1}{D_{BL}P_E^{3/2}} + \frac{28Q_V L_S / L_E}{\sigma_{BL}P_S^{3/2}} + \frac{L_S^2 / L_E^2}{D_{BL}P_S^{3/2}} + \frac{\tau_{SSD} + t_c}{L_E^2}\right]} \quad (8)$$

We note that, for reasons which will become clear, in equation (8) we have combined L_{AM} and D_{AM} in terms of the solid-state diffusion time, $\tau_{SSD} = L_{AM}^2 / D_{AM}$. Of the parameters within equation (8) the only ones that can vary significantly (i.e. by orders of magnitude) between electrodes are Q_V, L_E and τ_{SSD} and t_c. Typical values of Q_V vary between tens and thousands of mAh/cm^3 depending on the material, while the majority of electrodes would have thicknesses between 1 μm and a maximum of ~1 mm.[18] By analysing a large number of published papers, we recently showed that τ_{SSD} tends to fall in the range 1-10^4 s.[32] Finally, while t_c can be hard to pin down, Jiang et al.[9] have discussed values from 0.1-200 s. Of the other parameters, in real electrodes, the porosity tends to occupy a relative narrow range between ~0.4 and 0.6,[33] while the other parameters have reasonably standard values: σ_{BL}~0.5 S/m, D_{BL}~3×10^{-10} m^2/s, P_S~0.4, L_S~25 μm (although here, L_S=16 μm).[12]

To estimate the minimum electronic conductivity required to optimise rate-performance, we use equation (8) to plot $\sigma_{OOP,Min}$ in figure 5C as a contour plot versus Q_V and L_E using Q_V- and L_E-ranges as described above. We use the values of σ_{BL}, D_{BL}, P_S and L_S given above and take P_E=0.5. Considering the numbers above, we take a minimal values of $\tau_{SSD} + t_c$ = 1 s, as this

leads to higher values of $\sigma_{OOP,Min}$ than using the maximal value (see SI). This graph clearly shows that under almost any circumstances, an out-of-plane electronic conductivity of 1 S/m will be enough to render term 1 in equation (6a) negligible, and thus optimise rate-performance from a filler perspective. With reference to figure 2, attaining σ_{OOP}=1 S/m would require >10vol% (i.e. >12wt%) CB or graphene but <1vol% (<1.3wt%) carbon nanotubes.

This work shows that carbon nanotubes have significant advantages as conductive additives in battery electrodes. In the context of rate performance optimization, such fillers seem to allow efficient electron transfer through the electrolyte-soaked composite so that reactions with Li^+ occur more efficiently. Even at modest rates, electrolyte diffusion limitations can occur, but ensuring sufficient electron density at active material surface is still critical to ensure maximum lithiation for all proximal cations to active surfaces.

We believe this ability to remove electrical limitations is of great practical importance. It's potential can be seen in recent work by Gogotsi et al which demonstrated super-fast rate performance in supercapacitors using high conductivity MXene-based electrodes.[34] Similarly, Hersam et al achieved extraordinarily high rate-performance in battery electrodes by removing resistance limitations via conformal wrapping of active particles by graphene sheets.[35] The value of our work is that we provide an electronic conductivity target which allows the most efficient removal of electrical limitations.

3. CONCLUSIONS

In this work we have shown that composite battery electrodes of NMC filled with three different conductive additives, carbon black, graphene or carbon nanotubes, show significant electronic conductivity anisotropy, with out-of-plane conductivities (σ_{OOP}) roughly ×1000 lower than those measured in-plane. While carbon black or graphene loadings of >10wt% are required to reach OOP conductivities of 1 S/m, this level can be achieved with ~1wt% of carbon nanotubes. We found the rate-performance of such composite electrodes to depend strongly on filler loading. By fitting capacity-rate curves to an empirical equation, we extracted the characteristic charge/discharge time, τ, for each electrode. Informed by a simple mechanistic model, we found τ to scale approximately linearly with $1/\sigma_{OOP}$ for all materials. By plotting τ / L_E^2 , where L_E is the electrode thickness, versus Q_V / σ_{OOP} , where Q_V is the electrode volumetric capacity, we found all data to collapse onto a linear master curve. This curve agreed almost perfectly with the predictions of the model with no adjustable fitting parameters. This

allows us to use this model to estimate a minimum out-of-plane conductivity of 1 S/m required to optimise rate-performance.

This work highlights the importance of the out-of-plane conductivity to rate-performance in batteries and shows that conductivity measured in-plane is not a good metric for battery performance. It also shows that the loading level required to achieve sufficient electronic conductivity varies very strongly with filler type, with carbon nanotubes showing the greatest efficiency in this regard. In addition, we emphasise that simple mechanistic models can accurately predict experimental data without the need to perform complex simulations.

Finally, we highlight the fact that, although this work has been performed on lithium ion cathodes of a specific type, the associated physics (e.g. equation 6a) is general. This means the results obtained can be applied to both cathodes and anodes, not only of lithium ion batteries, but also batteries incorporating sodium and beyond.

4. METHODS

NMC811 powder was purchased from MTI Corporation and had a mean particle size of ~10 μm. Single walled nanotubes were purchased from OCSiAl (Tuball, 0.2 wt% CNT in NMP, 2wt% PVDF as a surfactant stabilizer). These nanotubes have mean lengths of ~5 μm and diameters in the range 1-2 nm and are very well graphitised. Graphene Powder was purchased from Tianyuan Empire and consisted of largely defect free flakes with thickness <5 layers and lengths in the range 1-5 μm. Carbon black (Timical Super C65) was purchased from MTI Corp and had an estimated particle radius of ~20 nm.

Samples for in-plane and out-of-plane conductivity measurements were prepared via the conventional slurry-casting method. $LiNi_{0.8}Co_{0.1}Mn_{0.1}O_2$ (NMC811) powder (MTI Corporation) was mixed with the respective conductive additive: CNTs, CB, Graphene, Polyvinylidene Fluoride (PVDF, EQ-Lib-PVDF, MTI Corp) and with sufficient amounts of N-Methyl-2-pyrrolidone (NMP) to form the slurry. There was 10wt% PVDF in most of the samples. However, the PDVF loading was increased to improve the Critic Crack Thickness (CCT)[18] of samples with extremely high loading of CB (18wt% and 22wt% PVDF in 15wt%CB and 20wt%CB samples). Samples for in-plane measurements were adhered to glass slides, whereas out-of-plane samples were cast onto an Al current collector using a doctor blade. All samples were dried overnight at 40 ^{o}C while the mass loading of active material

(NMC811) was kept roughly constant at ~15 mg cm^{-2} (mean 14 mg/cm^2, std dev 4 mg/cm^2). The electrodes thickness were roughly 100 μm (mean 96 μm, std dev 18μm).

Each in-plane sample was cut into a rectangular shape and silver wires were attached to the ends of the samples by painting them on with silver paint. This configuration allowed for intimate contact between sample and probe and in-plane conductivities were measured using the 2-point probe method. As for out-of-plane conductivity, circular disc electrodes with diameter = 12 mm were prepared by using a coin-cell disc puncher. Each electrode was then assembled into 2032-type coin cells in an Ar-filled glovebox (UNIlab Pro, Mbraun) in the following geometry: top, spring, two spacers, electrode, current collector, bottom. Out-of-plane conductivities were then measured using the two-point probe method. We expect the contact resistance between the top conductive spacer and the electrode to be non-trivial.

The electrochemical properties of the electrodes were measured in half cell (PAT-cell, EC Lab, BioLogic). All coin cells were assembled in an Ar-filled glovebox (UNIlab Pro, Mbraun). The dried electrodes were cut into 12 mm diameter discs and paired with Li metal discs (diameter= 16 mm). Celgard 2032 (thickness = 16 μm) was used as a separator. The electrolyte was 1.2 M $LiPF_6$ dissolved in EC/EMC (1:1 in v/v, BASF) with 10wt% Fluoroethylene carbonate (FEC). The tests were performed at a potentiostat (VMP3, Biologic). The GCD measurements (at I/A=17 mA/g) were performed for 2-3 cycles to form stable solid-electrolyte- interface (SEI) film in the half cells, and the voltage range was 3−4.3 V. After the capacities were stable, the cells were charged at I/A=17 mA/g [29]to 4.3 V, and CA measurements were performed for discharge at 3 V.[27] In this paper, all specific capacities are normalised to active electrode mass while the volumetric capacity is normalised to total electrode volume.

Acknowledgments: The authors acknowledge the SFI-funded AMBER research centre (SFI/12/RC/2278) and Nokia-Bell Labs for support. JNC thanks Science Foundation Ireland (SFI, 11/PI/1087) and the Graphene Flagship (grant agreement n°785219) for funding. COD acknowledges SFI under grant nos 14/IA/2581, 15/TIDA/2893 and the SmartVista project, which has received funding from the European Union's Horizon 2020 research and innovation programme under the grant agreement No. 825114.

The Supporting Information is available free of charge at https://pubs.acs.org/. Electrode density data, sample, charge-discharge curves, calculation details, model predictions.

FIGURES and TABLES

	In plane	Out of plane
Carbon black		
σ_0 (S/m)	1.35×10^4	4.50
ϕ_c (vol%)	0.9	0.7
t	1.99	1.5
Graphene		
σ_0 (S/m)	3.66×10^4	7.79
ϕ_c (vol%)	2.3	2.1
t	2.11	1.71
CNTS		
σ_0 (S/m)	1.35×10^8	6.2×10^4
ϕ_c (vol%)	0.01	0.01
t	2.0	1.87

Table 1: Percolation fit parameters found by fitting the data in figure 2 using equation (1).

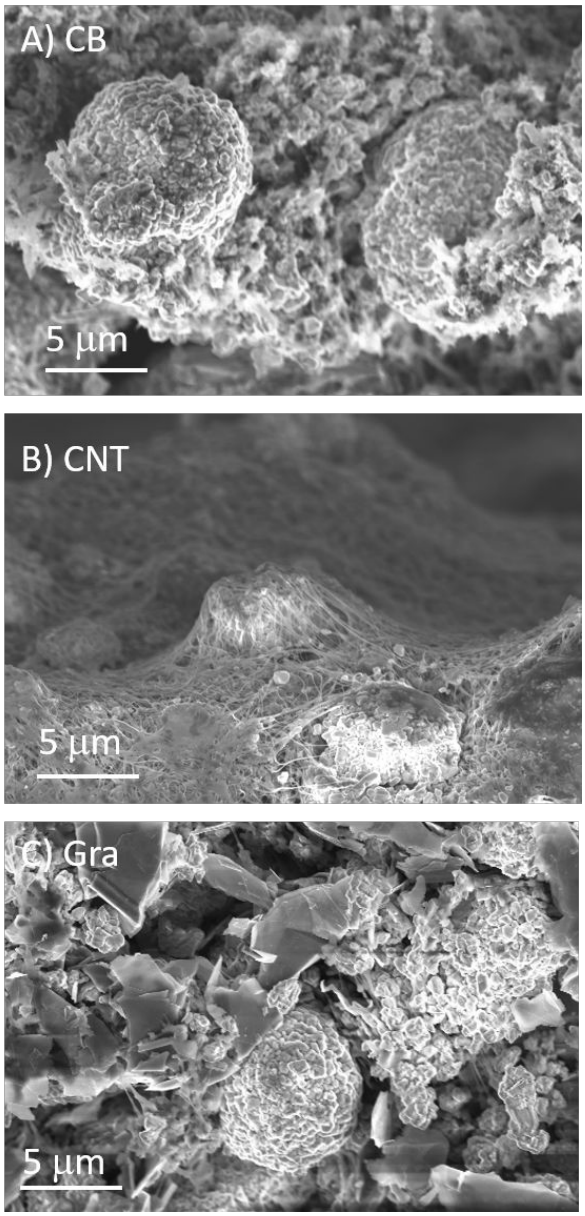

Figure 1: SEM images of fracture surfaces for A) 6wt% CB, B) 1wt% CNT, and C) 10wt% Graphene of each composite type.

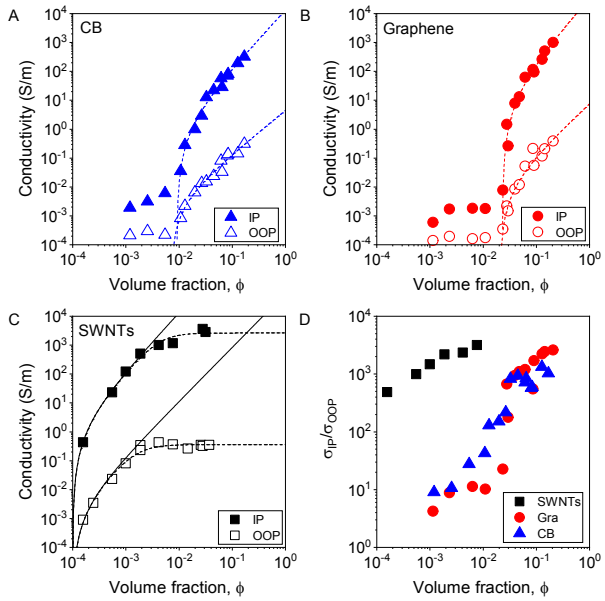

Figure 2: Conductivity of composite electrodes based on NMC811 filled with various conductive fillers. A-C) Measured conductivity as a function of volume fraction of conductive additives for composites filed with carbon black (A), graphene (B) and carbon nanotubes (C). The open symbols represent out-of-plane conductivity while the solid symbols represent in-plane conductivity. In A-C the dashed lines represent percolation fits (equation (1)). In C, the fits include the effect of contact resistance (equation (2b)). The solid lines represent the conductivity, estimated from the fits with the effect of contact resistance removed (i.e. using equation (1)). D) Ratio of in-plane to out of plane conductivity plotted versus volume fraction.

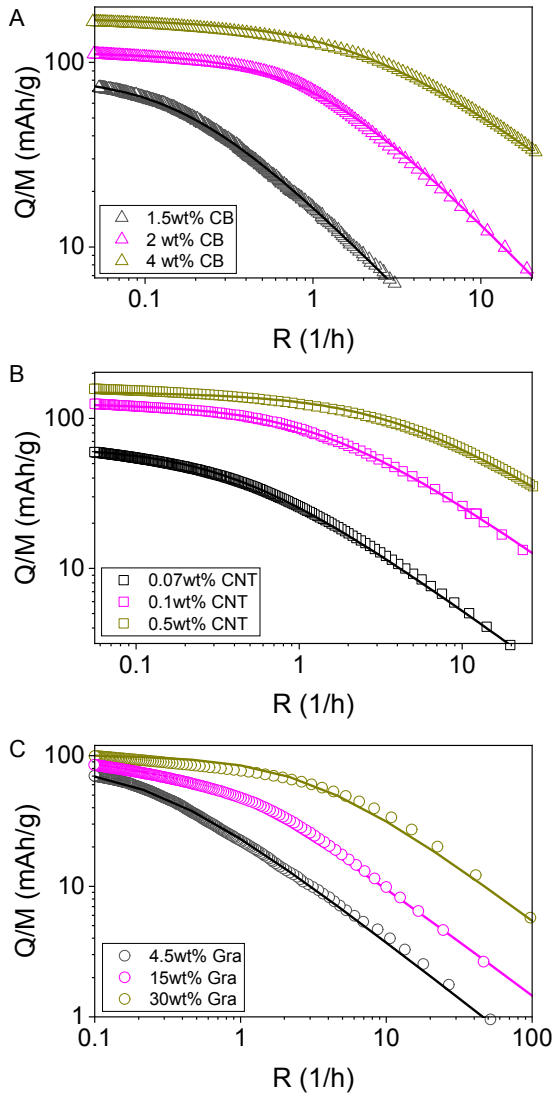

Figure 3: Rate-performance data for NMC811 electrodes incorporating carbon based conductive additives. A-C) Specific capacity (normalised to active mass) plotted versus rate NMC811-based electrodes filled with various loadings of carbon black (A), single-walled carbon nanotubes (B) and graphene (C). We note that these rates are equivalent to specific currents roughly in the range 5-500 mA/g.

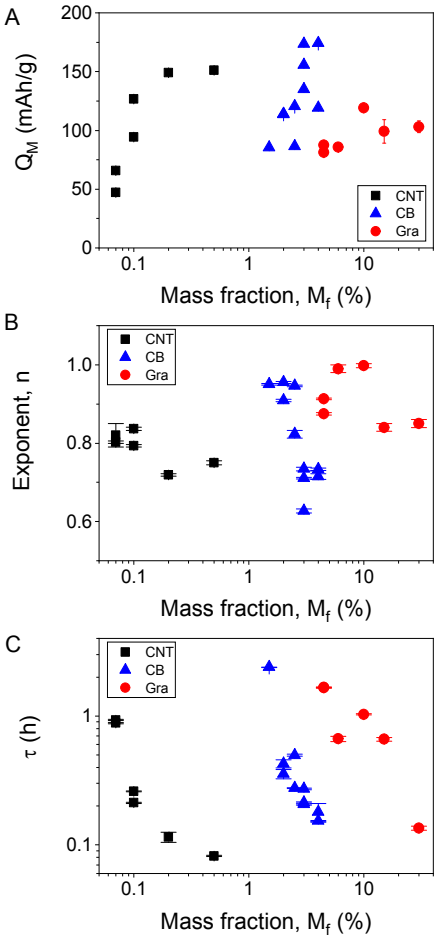

Figure 4: Rate-data fit parameters as a function of mass fraction of conductive additive. A) Low-rate specific capacity, QM, (B) characteristic time, τ, (C) and rate exponent, n, each plotted against mass fraction for all three types of conductive additive (single-walled carbon nanotubes, carbon black and graphene).

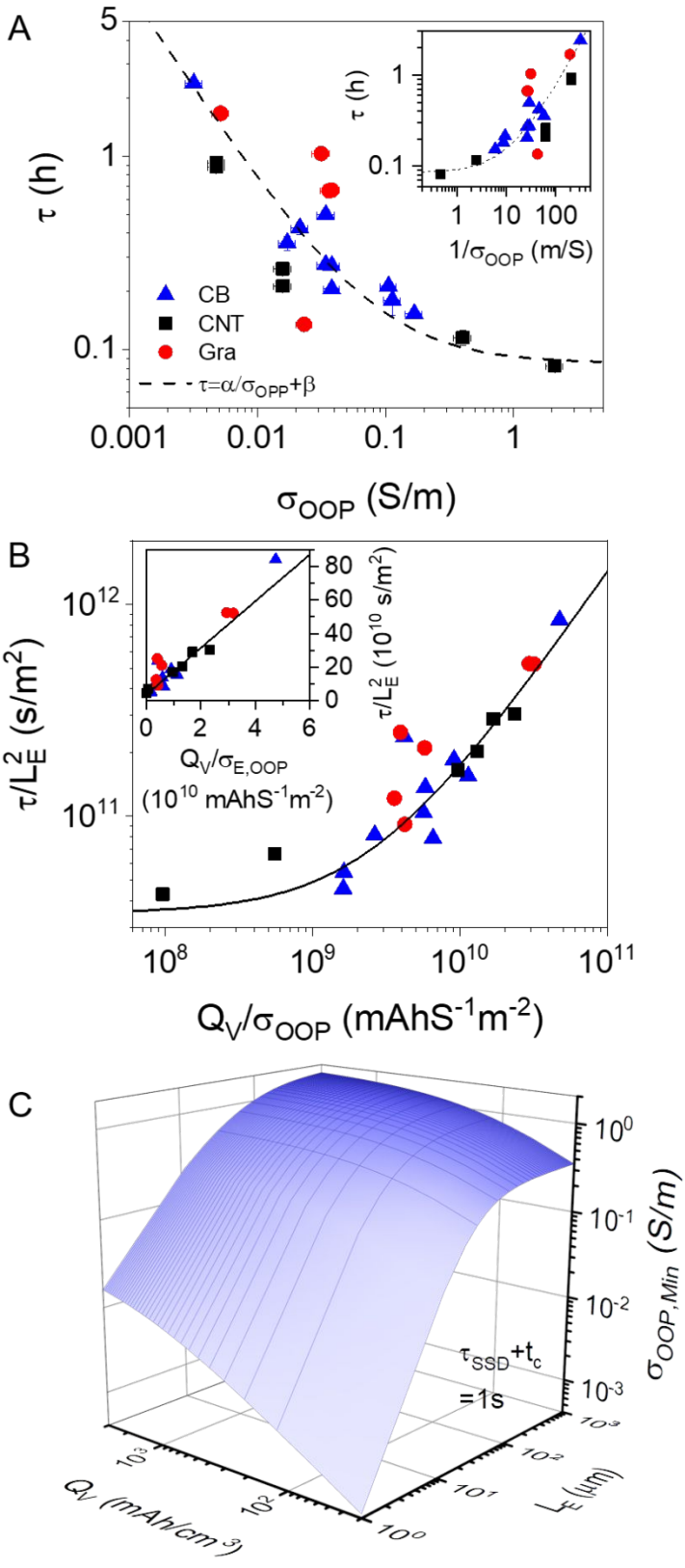

Figure 5: The effect of conductivity on rate-performance. A) Characteristic time, τ, plotted versus out-of-plane electrode conductivity, σ_{OOP}, for electrodes incorporating all three conductive additives (single-walled carbon nanotubes, carbon black and graphene). The dashed

line illustrates linearity between τ and $1/\sigma_{OOP}$. B) Characteristic time divided by electrode thickness squared (τ / L_E^2) plotted versus low-rate volumetric capacity divided by out-of-plane electrode conductivity (Q_V / σ_{OOP}). The solid line is a plot of equation (7) using the following parameters: $\langle Q_V \rangle$=2.1×10^8 mAh/m^3, σ_{BL}=0.5 S/m, D_{BL}=3×10^{-10} m^2/s, P_E=0.6, P_S=0.4, L_S=16 μm, $\langle L_E \rangle$=97 μm, L_{AM}=r/3=2μm, D_{AM}=5×10^{-14} m^2/s, t_c=25s (see SI for justification). C) Critical (out-of-plane) electrode conductivity, $\sigma_{OOP,min}$, plotted as a function of electrode thickness (L_E) and low rate volumetric capacity (Q_V). The critical conductivity is that required to reduce the contribution to τ associated with the electrode resistance (first term in equation (6a)) below 10% of the sum of the other contributions to τ (i.e. the other six terms in equation (6a)). Here we calculate $\sigma_{OOP,min}$ using the parameters given above and taking a short (τ_{SSD}+t_c=1s) combination of solid-state diffusion and reaction times.

TOC

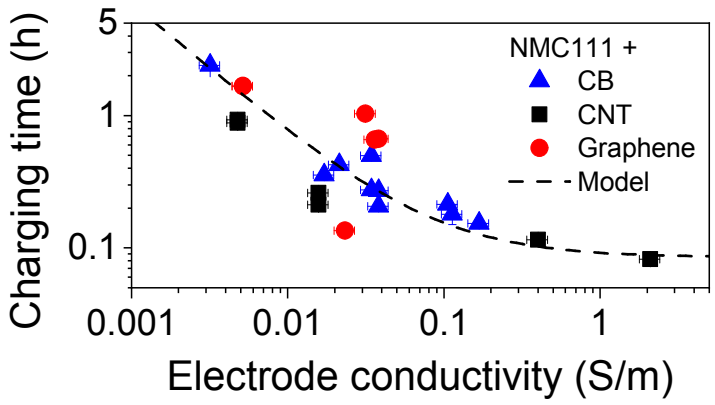

References

(1) Armand, M.; Tarascon, J. M. Building better batteries. *Nature* **2008,** *451*, 652-657.
(2) Wong, L. L.; Chen, H. M.; Adams, S. Design of fast ion conducting cathode materials for grid-scale sodium-ion batteries. *Phys. Chem. Chem. Phys.* **2017,** *19*, 7506-7523.
(3) Bonaccorso, F.; Colombo, L.; Yu, G. H.; Stoller, M.; Tozzini, V.; Ferrari, A. C.; Ruoff, R. S.; Pellegrini, V. Graphene, related two-dimensional crystals, and hybrid systems for energy conversion and storage. *Science* **2015,** *347*, 1246501.
(4) Ye, H. L.; Wang, L.; Deng, S.; Zeng, X. Q.; Nie, K. Q.; Duchesne, P. N.; Wang, B.; Liu, S.; Zhou, J. H.; Zhao, F. P.; Han, N.; Zhang, P.; Zhong, J.; Sun, X. H.; Li, Y. Y.; Li, Y. G.; Lu, J. Amorphous MoS3 Infiltrated with Carbon Nanotubes as an Advanced Anode Material of Sodium-Ion Batteries with Large Gravimetric, Areal, and Volumetric Capacities. *Adv. Energy Mater.* **2017,** *7*, 1601602.
(5) Lam, D.; Chen, K. S.; Kang, J.; Liu, X. L.; Hersam, M. C. Anhydrous Liquid-Phase Exfoliation of Pristine Electrochemically Active GeS Nanosheets. *Chem. Mater.* **2018,** *30*, 2245-2250.

(6) Marom, R.; Amalraj, S. F.; Leifer, N.; Jacob, D.; Aurbach, D. A review of advanced and practical lithium battery materials. *J. Mater. Chem.* **2011,** *21*, 9938-9954.
(7) Eftekhari, A. Lithium-Ion Batteries with High Rate Capabilities. *ACS Sustainable Chem. Eng.* **2017,** *5*, 2799-2816.
(8) Ye, J. C.; Baumgaertel, A. C.; Wang, Y. M.; Biener, J.; Biener, M. M. Structural Optimization of 3D Porous Electrodes for High-Rate Performance Lithium Ion Batteries. *ACS Nano* **2015,** *9*, 2194-2202.
(9) Jiang, F. M.; Peng, P. Elucidating the Performance Limitations of Lithium-ion Batteries due to Species and Charge Transport through Five Characteristic Parameters. *Sci. Rep.* **2016,** *6*, 32639.
(10) Zhang, H. G.; Yu, X. D.; Braun, P. V. Three-dimensional bicontinuous ultrafast-charge and -discharge bulk battery electrodes. *Nat. Nanotechnol.* **2011,** *6*, 277-281.
(11) Doyle, M.; Newman, J. Analysis of capacity-rate data for lithium batteries using simplified models of the discharge process. *J. Appl. Electrochem.* **1997,** *27*, 846-856.
(12) Tian, R.; Park, S.-H.; King, P. J.; Cunningham, G.; Coelho, J.; Nicolosi, V.; Coleman, J. N. Quantifying the factors limiting rate performance in battery electrodes. *Nature Commun.* **2019,** *10*, 1933.
(13) Zhang, Q. T.; Yu, Z. L.; Du, P.; Su, C. Carbon Nanomaterials Used as Conductive Additives in Lithium Ion Batteries. *Recent Pat. Nanotechnol.* **2010,** *4*, 100-110.
(14) Renteria, J. D.; Ramirez, S.; Malekpour, H.; Alonso, B.; Centeno, A.; Zurutuza, A.; Cocemasov, A. I.; Nika, D. L.; Balandin, A. A. Strongly Anisotropic Thermal Conductivity of Free-Standing Reduced Graphene Oxide Films Annealed at High Temperature. *Adv. Funct. Mater.* **2015,** *25*, 4664-4672.
(15) Gabbett, C.; Boland, C. S.; Harvey, A.; Vega-Mayoral, V.; Young, R. J.; Coleman, J. N. The Effect of Network Formation on the Mechanical Properties of 1D:2D Nano:Nano Composites. *Chem. Mater.* **2018,** *30*, 5245-5255.
(16) Liu, Y. P.; He, X. Y.; Hanlon, D.; Harvey, A.; Khan, U.; Li, Y. G.; Coleman, J. N. Electrical, Mechanical, and Capacity Percolation Leads to High-Performance MoS2/Nanotube Composite Lithium Ion Battery Electrodes. *ACS Nano* **2016,** *10*, 5980-5990.
(17) Zhang, B.; Yu, Y.; Liu, Y. S.; Huang, Z. D.; He, Y. B.; Kim, J. K. Percolation threshold of graphene nanosheets as conductive additives in Li4Ti5O12 anodes of Li-ion batteries. *Nanoscale* **2013,** *5*, 2100-2106.
(18) Park, S. H.; King, P. J.; Tian, R. Y.; Boland, C. S.; Coelho, J.; Zhang, C. F.; McBean, P.; McEvoy, N.; Kremer, M. P.; Daly, D.; Coleman, J. N.; Nicolosi, V. High areal capacity battery electrodes enabled by segregated nanotube networks. *Nat. Energy* **2019,** *4*, 560-567.
(19) Zhang, C. F.; Park, S. N.; Seral-Ascaso, A.; Barwich, S.; McEyoy, N.; Boland, C. S.; Coleman, J. N.; Gogotsi, Y.; Nicolosi, V. High capacity silicon anodes enabled by MXene viscous aqueous ink. *Nature Commun.* **2019,** *10*, 849.
(20) Celzard, A.; Mareche, J. F.; Furdin, G.; Puricelli, S. Electrical conductivity of anisotropic expanded graphite-based monoliths. *J. Phys. D: Appl. Phys.* **2000,** *33*, 3094-3101.
(21) Glynn, C.; Thompson, D.; Paez, J.; Collins, G.; Benavente, E.; Lavayen, V.; Yutronic, N.; Holmes, J. D.; Gonzalez, G.; O'Dwyer, C. Large directional conductivity change in chemically stable layered thin films of vanadium oxide and a 1D metal complex. *J. Mater. Chem. C* **2013,** *1*, 5675-5684.
(22) Bauhofer, W.; Kovacs, J. Z. A review and analysis of electrical percolation in carbon nanotube polymer composites. *Compos. Sci. Technol.* **2009,** *69*, 1486-1498.
(23) White, S. I.; DiDonna, B. A.; Mu, M. F.; Lubensky, T. C.; Winey, K. I. Simulations and electrical conductivity of percolated networks of finite rods with various degrees of axial alignment. *Phys. Rev. B* **2009,** *79*, 024301.
(24) Sole, C.; Drewett, N. E.; Liu, F.; Abdelkader, A. M.; Kinloch, I. A.; Hardwick, L. J. The role of re-aggregation on the performance of electrochemically exfoliated many-layer graphene for Li-ion batteries. *J. Electroanal. Chem.* **2015,** *753*, 35-41.
(25) Fan, X. L.; Chen, L.; Borodin, O.; Ji, X.; Chen, J.; Hou, S.; Deng, T.; Zheng, J.; Yang, C. Y.; Liou, S. C.; Amine, K.; Xu, K.; Wang, C. S. Non-flammable electrolyte enables Li-metal batteries with aggressive cathode chemistries. *Nat. Nanotechnol.* **2018,** *13*, 715-+.

(26) Heubner, C.; Lammel, C.; Nickol, A.; Liebmann, T.; Schneider, M.; Michaelis, A. Comparison of chronoamperometric response and rate-performance of porous insertion electrodes: Towards an accelerated rate capability test. *J. Power Sources* **2018,** *397*, 11-15.
(27) Ruiyuan Tian; Paul J. King; Joao Coelho; Sang-Hoon Park; Valeria Nicolosi; Colm O'Dwyer; Coleman, J. N. Using chronoamperometry to rapidly measure and quantitatively analyse rate performance in battery electrodes. *ArXiv 1911.12305* **2019**.
(28) Park, S.-H.; Tian, R.; Coelho, J.; Nicolosi, V.; Coleman, J. N. Quantifying the Trade-Off between Absolute Capacity and Rate Performance in Battery Electrodes. *Adv. Energy Mater.* **2019,** 1901359.
(29) Coleman, J.; Tian, R. Developing models to fit capacity-rate data in battery systems. *Current Opinion in Electrochemistry* **2020,** *21*, 1-6.
(30) Jow, T. R.; Delp, S. A.; Allen, J. L.; Jones, J.-P.; Smart, M. C. Factors Limiting Li+ Charge Transfer Kinetics in Li-Ion Batteries. *J. Electrochem. Soc.* **2018,** *165*, A361-A367.
(31) Heubner, C.; Schneider, M.; Michaelis, A. Diffusion-Limited C-Rate: A Fundamental Principle Quantifying the Intrinsic Limits of Li-Ion Batteries. *Adv. Energy Mater.* **2020,** *10*, 1902523.
(32) Ruiyuan Tian; Madeleine Breshears; Horvath, D. V.; Coleman, J. N. Is the Rate Performance of 2D Material-Based Battery Electrodes as Good as Commonly Believed? *ACS Nano* **2019,** *in press*.
(33) Chung, D. W.; Ebner, M.; Ely, D. R.; Wood, V.; Garcia, R. E. Validity of the Bruggeman relation for porous electrodes. *Modelling and Simulation in Materials Science and Engineering* **2013,** *21*, 074009.
(34) Lukatskaya, M. R.; Kota, S.; Lin, Z. F.; Zhao, M. Q.; Shpigel, N.; Levi, M. D.; Halim, J.; Taberna, P. L.; Barsoum, M.; Simon, P.; Gogotsi, Y. Ultra-high-rate pseudocapacitive energy storage in two-dimensional transition metal carbides. *Nat. Energy* **2017,** *2*, 17105.
(35) Chen, K. S.; Xu, R.; Luu, N. S.; Secor, E. B.; Hamamoto, K.; Li, Q. Q.; Kim, S.; Sangwan, V. K.; Balla, I.; Guiney, L. M.; Seo, J. W. T.; Yu, X. K.; Liu, W. W.; Wu, J. S.; Wolverton, C.; Dravid, V. P.; Barnett, S. A.; Lu, J.; Amine, K.; Hersam, M. C. Comprehensive Enhancement of Nanostructured Lithium-Ion Battery Cathode Materials via Conformal Graphene Dispersion. *Nano Lett.* **2017,** *17*, 2539-2546.